A System-on-Chip Digital pH Meter for Use in a Wireless Diagnostic Capsule

Paul A. Hammond*, Danish Ali, and David R. S. Cumming, *Member, IEEE*

***Abstract*—This paper describes the design and implementation of a system-on-chip digital pH meter, for use in a wireless capsule application. The system is organized around an 8-bit microcontroller, designed to be functionally identical to the Motorola 6805. The analog subsystem contains a floating-electrode ISFET, which is fully compatible with a commercial CMOS process. On-chip programmable voltage references and multiplexors permit flexibility with the minimum of external connections. The chip is designed in a modular fashion to facilitate verification and component re-use. The single-chip pH meter can be directly connected to a personal computer, and gives a response of 37 bits/pH, within an operating range of 7 pH units.**

***Index Terms*—CMOS, ISFET, pH, system-on-chip.**

I. Introduction

OVER the past twenty years there has been a drive in the electronics industry to connect an ever increasing number of components together at the integrated circuit level. This "system-on-chip" evolution has led to an increase in complexity, coupled with a reduction in size, cost, and power consumption of devices such as mobile telephones. CMOS is the dominant technology for system-on-chip devices, and for integrated circuits in general. In order to exploit the ubiquitous nature of CMOS chips, there have been many initiatives to fabricate chemical sensors in compatible technologies [1]. Most notably, a gas sensor which includes micro-machined resonating beams and digital interface electronics, has been integrated into a single CMOS chip [2].

An important developing application area for sensor systems is *in vivo* diagnostic devices. Capsule-based devices have been used to diagnose conditions of the gastro-intestinal (GI) tract. Conventional methods of measuring inside the GI tract require the passage of tubes through the throat or anus. Not only are these unpleasant procedures for the patient, but the physical presence of the tube can affect the phenomenon being studied. A device that could be swallowed and would transmit the required measurements without wires, from inside the patient is clearly desirable. In terms of pH measurement, tethered capsules have been employed most successfully to diagnose gastro-esophageal reflux disease (GERD) [3]. pH measurements from "flow-through" capsules have also been used to study inflammatory bowel diseases (IBDs) such as Crohn's disease and ulcerative colitis [4], [5]. In cows, data-logging pH-capsules have been used to measure the effect of diet on subclinical rumen acidosis, a common condition in dairy cattle [6]. A description of the fabrication and packaging of a multichannel wireless capsule, which includes a pH sensor, has recently been provided [7].

All of these pH-capsules used discrete sensors and components, connected together at the printed circuit board level. By designing a CMOS-compatible pH sensor, it may be integrated into a system-on-chip, producing the same cost, size, and power benefits for the capsule-based device. In the future, the system-on-chip could be reused as a platform for other integrated sensors to measure temperature, conductivity and other parameters. The solid-state pH sensor, being based on the ion-sensitive field-effect transistor (ISFET), is an ideal candidate for integration with the CMOS process. Recently, ISFETs have been fabricated in an unmodified commercial process, but were found to suffer from large and unpredictable threshold voltages [8]. This problem has been attributed to trapped charge, which can be removed using ultra-violet radiation [9]. In this paper, the idea of the CMOS ISFET is extended to a complete system-on-chip digital pH meter, ideal for use in a capsule-based diagnostic device, but with many other potential applications. Section II describes the overall system and the design of the digital and analog subsystems. Section III provides details of the packaging and experimental setup used to test the chip. Section IV gives results for the individual ISFET as well as the complete system both on the bench and in solution. Finally, Section V offers some conclusions.

II. System-on-Chip Design

A block diagram of the system-on-chip pH meter is shown in Fig. 1. The complete system is designed to collect and process pH data, and to communicate its results to the outside world via an off-chip radio transmitter. The system is controlled by a microcontroller unit (MCU), which obtains pH readings from the sensor block, and can store them in memory (SRAM) or pass them to the transmitter.

This project used a commercial 0.6 μm, three-metal CMOS process from austriamicrosystems AG (AMS). Where possible, the system was designed using existing components such as digital gates and operational amplifiers from the AMS design libraries. In addition, the system was constructed in a

Manuscript received March 5, 2004; revised September 12, 2004. This work was supported in part by grants from the Engineering and Physical Sciences Research Council (EPSRC), the Scottish Higher Education Funding Council (SHEFC), and from Philips Research Laboratories, UK. *Asterisk indicates corresponding author.*

*P. A. Hammond is with the Department of Electronics and Electrical Engineering, University of Glasgow, Glasgow G12 8LT, U.K. (e-mail: p.hammond@elec.gla.ac.uk).

D. Ali is with Philips Research Laboratories, Redhill RH1 5HA, UK.

D. R. S. Cumming is with the Department of Electronics and Electrical Engineering, University of Glasgow, Glasgow G12 8LT, U.K.

Digital Object Identifier 10.1109/TBME.2005.844041

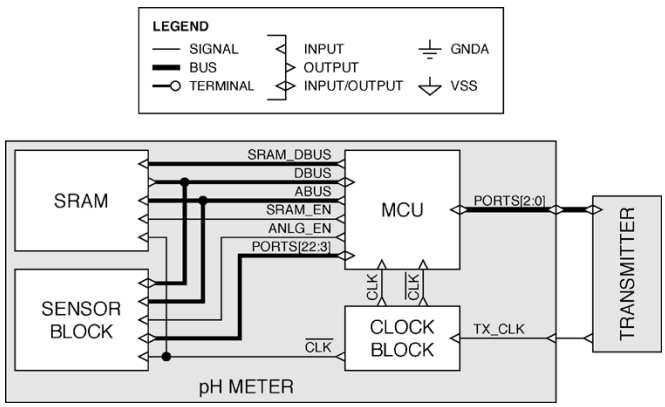

Fig. 1. Block diagram of the complete system-on-chip pH meter showing connection to an external transmitter chip.

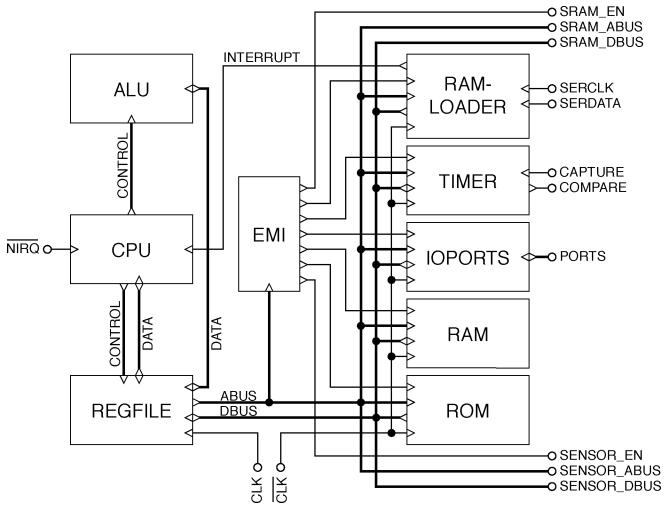

Fig. 2. Block diagram of the modified 6805 microcontroller showing the additional RAMLOADER block. (See Fig. 1 for legend.).

modular fashion, allowing individual blocks and subsystems to be re-used in future projects. These are important factors in system-on-chip methodology as they allow complicated devices to be designed quickly, using components that have already been verified.

A. The Digital Subsystem

In order to manage the behavior of the system, some form of digital control was required. Instead of using a custom logic circuit tailored to suit this chip, a more generic microcontroller was implemented, to provide flexibility during development and testing. The Motorola MC68HC05 MCU was selected as the controller to use, as it has a relatively simple architecture and small instruction set, and development tools and documentation are readily available. A model of the MC68HC05, or 6805 for short, was written in the hardware-description language VHDL.

The standard Motorola 6805 MCU stores its program code in EPROM so that it can be modified during development. There is no EPROM module available from the AMS foundry, but there are SRAM and ROM modules available. Rather than commit to a fixed program stored in ROM, it was decided to store the program code in SRAM. To make this possible it was necessary to add a "boot-from-link" function to the MCU. Several additions to the standard 6805 model were required to achieve this. First, a RAMLOADER block (Fig. 2) was designed to load serial data into an 8-bit shift register using external clock and data signals (SERCLK and SERDATA). When the register is full, the block raises an interrupt to inform the CPU that it should collect the data. The memory map of the 6805 also had to be modified to accommodate the boot-from-link interrupt routine. This routine, which is hard-coded in ROM, is triggered by the interrupt signal and copies the contents of the shift register into the SRAM. Four new instructions were added to the 6805 instruction-set to perform the boot-from-link process. The most important of these is the software reset, which allows the MCU to reset and begin execution of the newly downloaded program.

If the microchip is to be used in a capsule-based diagnostic application, it must have some means of communicating its data to a system outside of the subject's body. Extensive finite-difference time-domain (FDTD) simulations of an ingested transmitter have shown that maximum radiation occurs at frequencies in the range of 450–900 MHz [10]. This is close to the unlicensed industrial, scientific and medical (ISM) transmission bands at 433 MHz in Europe and 915 MHz in the United States. AMS produce a 433 MHz single-chip transmitter in a very small (3.8 mm by 4.8 mm by 1.3 mm) package. In principle, as it is produced by the same foundry, the intellectual property (IP) for this device could be licensed and included as part of the system-on-chip. However, to reduce the effects of high-frequency interference, it is common practice to keep the RF transmitter off-chip. There a large number of manufacturers producing miniature single-chip ISM transmitters, with simple 3-signal (clock, data, and control) interfaces. For this reason, three pins from the MCUs input/output ports were reserved for communication with an off-chip transmitter. The remaining pins were required on-chip to control the behavior of the analog subsystem to receive the pH measurement data.

Once the VHDL model had been written it was compiled, simulated and debugged using the Synopsys VHDL tool-set. When the model had been shown to perform as required, it was synthesized to create a structural netlist. The synthesis process automatically generates the details of the digital gates and their interconnections, which are required to perform the function of the VHDL model. After synthesis, the netlist was converted into a physical design using the Cadence Silicon Ensemble "place-and-route" tool. This created the layout data that was used to fabricate the MCU block that can be seen in Fig. 10.

B. The Analogue Subsystem

Fig. 3 shows the analog subsystem that was designed to convert the solution pH into an 8-bit value, which could be read by the microcontroller. The sensing element of the subsystem is an ion-sensitive FET (ISFET), whose threshold voltage varies with pH. The BIAS_CIRCUIT block sets the current for the ISFET_CIRCUIT, which in turn outputs the source voltage of the ISFET to the instrumentation amplifier block AGIA. The amplified signal is then passed to the analog-to-digital convertor (ADC), which provides the microcontroller with an 8-bit value.

The analog subsystem's need for external signals was eliminated by the use of programmable voltage references to set the bias currents, to drive a reference electrode, and to provide

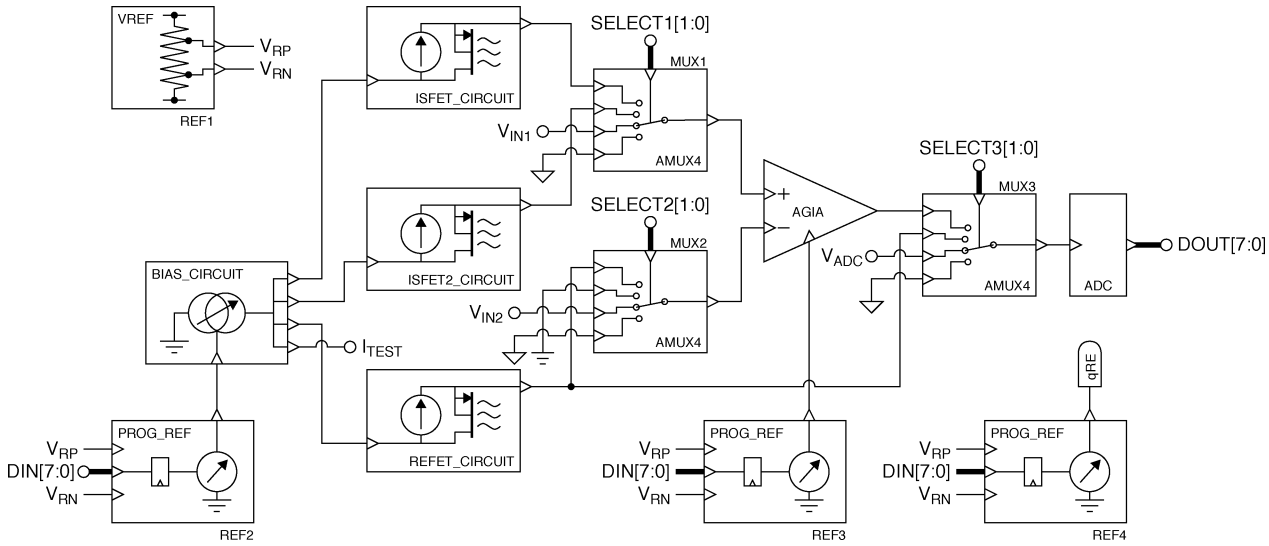

Fig. 3. Block diagram of the analog subsystem used to convert the solution pH into an 8-bit digital reading. (See Fig. 1 for legend, and note that the analog ground voltage GNDA is midway between the power supply voltages VDD and VSS.).

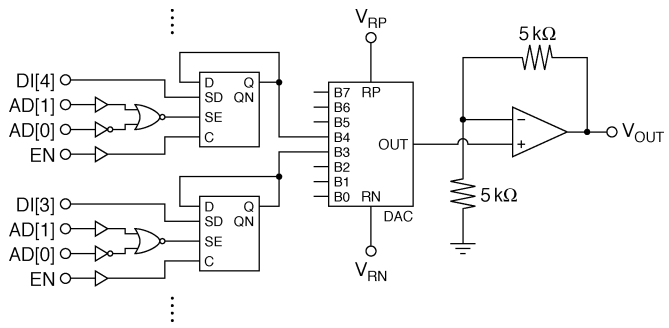

Fig. 4. Circuit diagram of the programmable voltage reference (PROG_REF).

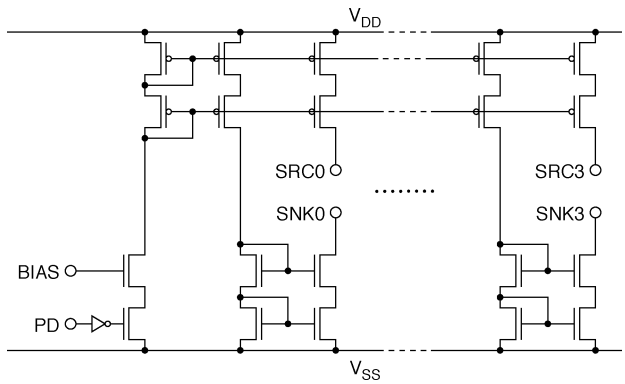

Fig. 5. Circuit diagram of the cascode-mirror current bias block (BIAS_CIRCUIT).

a "zeroing" voltage to the instrumentation amplifier. Analogue multiplexors (AMUX4) were included to allow selection between two different ISFET circuits, and to allow pH measurement either using a reference FET (REFET) or an external reference electrode. The multiplexors also include test inputs (V_{IN1}, V_{IN2}, and V_{ADC}) that were used during the initial system verification. There is also an extra output I_{TEST} from the BIAS_CIRCUIT that was used to calibrate the current mirrors. The analog subsystem is controlled by, and provides its pH readings via, the dedicated input/output ports of the MCU. As well as controlling the switching of the multiplexors, the MCU is able to selectively power-down any unused blocks.

The programmable voltage references (PROG_REF) shown in Fig. 4, each contain a memory-mapped register, a digital-to-analog convertor (DAC), and an operational amplifier (op-amp). The register comprises eight scannable flip-flops and some address-decode logic. A new value is loaded from the scan data 'SD' pin when the scan enable "SE" signal is high. Otherwise, the data is reloaded from the "Q"-"D" feedback loop each time the enable signal "EN" is high. Note that the logic is sufficiently simple that the scan inputs are not required for their conventional use in a scan-chain. The output "Q" terminals of the flip-flops are also connected to the input of an 8-bit DAC. The gain of the amplifier stage, which follows the DAC, was chosen to increase the output range to 0.5–4.5 V, which covers 10%–90% of the supply voltage. The DAC, the flip-flops, and the op-amp are all standard AMS library components.

The BIAS_CIRCUIT (Fig. 5) block contains a cascode current mirror with four pairs of source/sink outputs to provide a constant current to the ISFET_CIRCUIT blocks. The current is set by the voltage on the "BIAS" terminal, and the complete mirror can be switched off via the "PD" terminal. The AMUX4 blocks are conventional 4-to-1 analog multiplexors created using NMOS and PMOS pairs as pass-gates. AGIA is a standard three op-amp instrumentation amplifier, but the potential at the ground reference terminal can be adjusted to zero the output voltage.

Inside the ISFET_CIRCUIT block (Fig. 6, [11]), the drain-source voltage V_{DS} of the ISFET is held fixed by a pair of op-amps and a 5 kΩ resistor. Both op-amps are connected as unity-gain buffers and output a voltage equal to that on their noninverting $(+)$ inputs. The current source SRC0 provides a constant 100 μA current I_D to the source terminal of the ISFET. Op-amp A1 outputs the source voltage V_S to the top terminal of the 5 kΩ resistor. The current sink SNK0 draws 100 μA through the resistor, developing a potential drop of 0.5 V. Op-amp A2 outputs the potential of the bottom resistor terminal to the drain

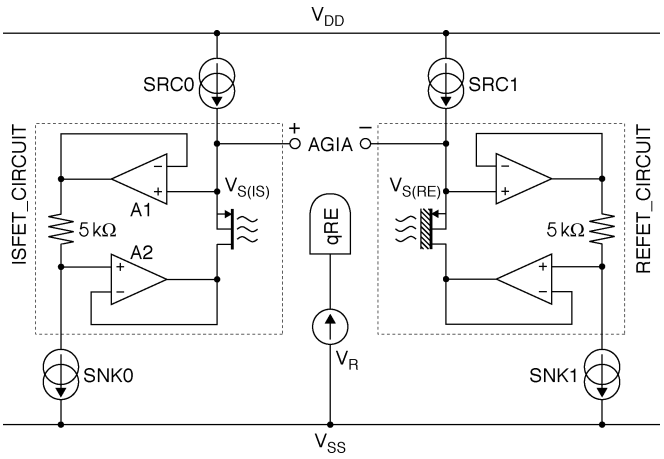

Fig. 6. Circuit diagram of the differential pH-measurement circuit.

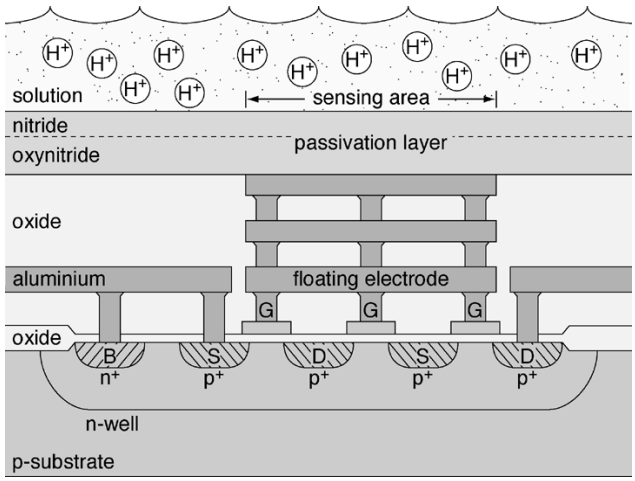

Fig. 7. Diagram of the cross-section through a p-type floating-electrode CMOS ISFET.

terminal of the ISFET. This loop ensures that a constant drain-source potential difference of 0.5 V is maintained.

ISFET circuits are usually biased using a reference electrode, that provides a constant electrode/solution potential difference. Such electrodes require an internal reference solution separated from the test solution by a permeable membrane. Miniature $\mathrm{Ag|AgCl}$ reference electrodes have been fabricated, but they require relatively complicated processing techniques [12], [13]. As an alternative, a REFET and a stable metal quasi-reference electrode (qRE) may be used. A REFET may be simply formed by the application of a suitable polymer membrane to the surface of an ISFET [14], [15]. The REFET_CIRCUIT is biased using SRC1, SNK1 and forms the other half of the differential circuit shown in Fig. 6. This arrangement allows both ISFET and REFET to be biased using a single qRE. Since both SRC0, SRC1 and SNK0, SNK1 are parts of the same current mirror, both ISFET and REFET will be biased at identical operating points. Changes in solution potential, temperature and power-supply voltage affect both ISFET and REFET equally, so can be rejected as a common-mode signal by the amplifier AGIA. In order for this to work, the REFET must have identical electrical characteristics to the ISFET, while having a very low (ideally zero) pH sensitivity.

It is necessary to maintain both constant drain current and constant drain-source voltage in the ISFET, in order to detect changes in its threshold voltage, a quantity which is not directly measurable. For an ISFET operating in the saturation region, the drain current is given by

$$I_D = \frac{k'}{2}\frac{W}{L}(V_{RS} - V_T)^2(1 + \lambda V_{DS}) \qquad (1)$$

where k' is a process-dependant constant, λ is the channel-length modulation factor, and W and L are the width and length of the channel. V_S and V_D are the source and drain terminal voltages, and V_R is the applied reference electrode voltage. Both I_D and V_{DS} are held constant by the circuit, so $(V_{RS} - V_T)$ must also remain constant. As the threshold voltage V_T varies with changing solution pH, V_{RS} must adjust by an equal amount to compensate. Since the reference electrode voltage V_R is also fixed, changes in V_T are tracked by changes in the source voltage V_S, providing a measurable output.

The ISFET itself employs a floating-electrode design, allowing the passivation layer to act as the pH-sensitive insulator [8]. In the CMOS process used, the passivation layer consists of 0.4 μm of silicon nitride on top of 0.6 μm of silicon oxynitride, deposited by plasma-enhanced chemical vapor deposition (PECVD). Silicon nitride is a well-known material for ISFET fabrication and gives a linear pH-response with a sensitivity in the range of 45–56 mV/pH [16]. The polysilicon layer and the three metal layers are connected together using vias to form a floating electrode. Since the substrate is p-type silicon, a p-type ISFET is formed in an n-type well. This allows the bulk terminal to be connected directly to the source $(V_{BS} = 0)$ so that a change in source potential does not affect the threshold voltage. It also means that the ISFET is isolated from the rest of the chip by a reverse-biased diode between the well and the substrate. The source and drain regions of the ISFET were interleaved as shown in Fig. 7. The properties of an ISFET fabricated using this method have been described elsewhere [9]. The ISFET2_CIRCUIT block (Fig. 3) uses an ISFET with its floating electrode connected to a small pad for test purposes.

III. Experimental

The system-on-chip pH meter was fabricated and supplied as both packaged and unpackaged chips. The packaged chips were used for initial verification and to develop the program code. A specially designed PCB was used to provide access to all 68 pins. A waveform generator provided a 1–MHz clock signal to the chip, and a logic analyzer monitored activity on the address and data buses. For simplicity during testing, the transmitter interface of the chip (Fig. 1) was connected directly to the parallel port of a PC. Software running on the PC was used to download program code to the chip and to upload the results of experiments. The program code itself was written and simulated in 6805 assembly language, then compiled into machine code. This machine code was then converted into a list of 2048 bytes ready for download into the SRAM.

The download software simply uses a timer function to provide both clock and serial data to the BOOTLOADER block. However, the upload software requires synchronization between

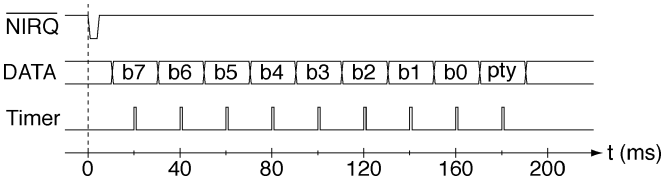

Fig. 8. Timing diagram for the interrupt-controlled data upload process from chip to PC.

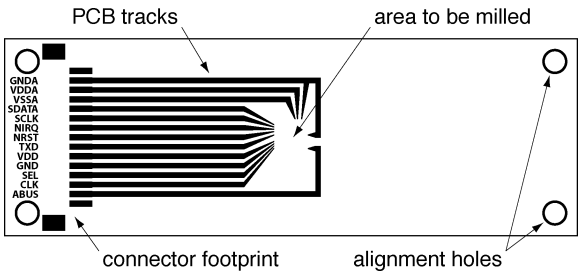

Fig. 9. Diagram of the mask used to create the PCB for in-solution testing (shown actual size).

the parallel port and the chip, which do not share a common clock. To achieve this, the interrupt-driven scheme shown in Fig. 8 was implemented. To upload one byte of data, the PC first drives a "0" onto the NIRQ signal, which triggers an interrupt. The MCU begins by transmitting the first data bit on the DATA signal, after an initial delay of 10 ms. The remaining seven data bits, plus a final parity bit, are transmitted at 20-ms intervals. The MCU generates the 10- and 20-ms delays using `do...while` loops. The timer function of the uploader software loads nine bits from the parallel port, one every 20 ms after the interrupt has been triggered. Ideally this would mean that the software samples the 'DATA' signal exactly midway between transitions as shown in Fig. 8. However, even a 10% discrepancy between PC and MCU timings will not cause the wrong bit to be sampled. Another interrupt is required to upload the next byte, allowing the MCU and the PC to regain synchronization.

Before the unpackaged chips could be tested in solution they had to be wire-bonded and encapsulated in a PCB. Since most of the 68 pins are for debugging purposes, it was only necessary to use 14 pins for in-solution testing. These comprise pins for the (separated) analog and digital power supplies, the chip reset, the program download and data upload interfaces, an external clock, and the most-significant bit of the address bus. This last signal changes frequently and provides an indicator of system activity. A diagram of the mask used to create the PCB is shown in Fig. 9. A recess measuring 4.5 mm by 4.75 mm and 580 μm deep was milled into the centre of the PCB using a high-speed (60 000 rpm) milling machine. Before the chip was glued into the recess, it was placed in an EPROM eraser for 24 h to reduce the ISFET threshold voltage [9]. The relevant bond-pads on the chip were then wire-bonded to PCB tracks and the whole assembly was encapsulated with SU-8 photoresist, using a process described elsewhere [17]. A photomicrograph of the encapsulated chip, showing the ISFET exposed by a well in the photoresist, is shown in Fig. 10.

After the chip had been encapsulated, it was placed in a beaker of solution with a conventional Ag|AgCl reference

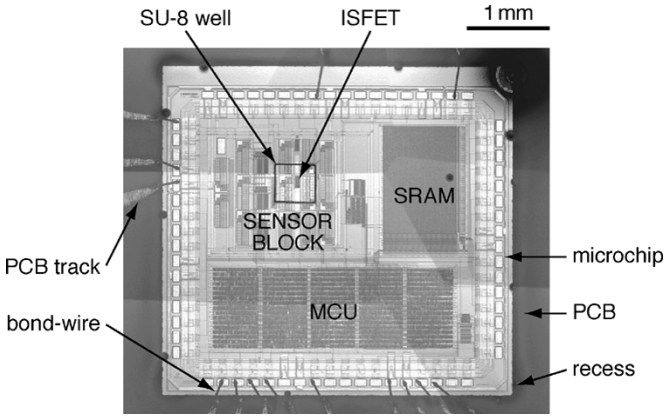

Fig. 10. Photomicrograph of the encapsulated system-on-chip pH meter showing ISFET exposed through a 500 μm square well in the SU-8 photoresist.

electrode. A solution of 0.15 M sodium chloride with a 0.01 M pH 7 phosphate buffer was chosen to simulate physiological fluids. Metered quantities of 1 M HCl were added with an adjustable pipette, to reduce the pH of the solution. A magnetic stirrer was used to ensure rapid and complete mixing of the solution when the acid was added. The solution pH was measured with a Hanna pH 211 meter and a Sentron IntelliProbe Hot-Line CupFET probe. To avoid electrical interference from placing the probe in solution, a small sample of the solution was removed using a glass pipette and placed onto the probe.

IV. Results and Discussion

A. Individual ISFET and REFET Devices

The pH sensitivity of individual ISFETs was measured using a version of the circuit shown in Fig. 6, made from discrete components. The reference electrode voltage, and the source and sink bias currents were provided by source-measure units (SMUs) of a Keithley 4200-SCS semiconductor parameter analyzer. The effect of solution pH on the ISFET threshold voltage is clearly seen in Fig. 11(a). After 10 min 500 μl of 1 M HCl was added, reducing the pH from 6.77 to 3.47.

Threshold voltage drift [9] is also present, in fact it has a larger effect over 20 min than does the change in pH. Threshold voltage drift for silicon nitride ISFETs has been successfully modeled by a "stretched-exponential" time dependence [18]. Upon exposure to an aqueous solution, silicon nitride forms a thin hydrated layer as hydrogen ions diffuse into the material by a mechanism known as "dispersive transport" [19]. The growth of a modified surface layer affects the overall insulator capacitance, which in turn affects the threshold voltage. Since the layer thickness has a stretched-exponential time dependence, so too will the threshold voltage drift

$$\Delta V_T(t) = \Delta V_T(\infty)\left\{1 - \exp\left[-\left(\frac{t}{\tau}\right)^{\beta}\right]\right\} \qquad (2)$$

where $\Delta V_T(\infty)$ is the ultimate change in threshold voltage as a result of drift. τ is the time constant, and β the dispersion parameter, characterising the dispersive transport of hydrogen [19]. A nonlinear curve-fitting algorithm (Levenberg–Marquardt, [20]) was used to fit (2) to the first 550 s of data in

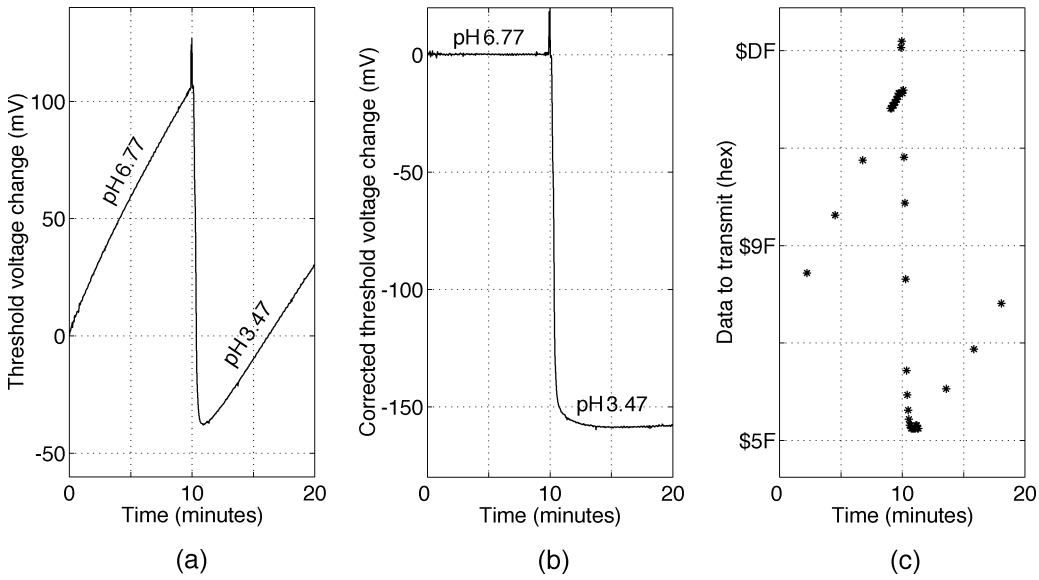

Fig. 11. Graphs of the ISFET threshold voltage response to a change in solution pH, (a) as measured, (b) with the Levenberg–Marquardt drift correction applied, and (c) with a simple linear predictor used as drift compensation.

Fig. 11(a). The modeled drift for the whole 20 min was then subtracted from the measured data to produce the "corrected" pH response shown in Fig. 11(b). The threshold voltage changes by approximately -159 mV for a change in pH of -3.3 units, giving an ISFET pH-sensitivity of 48 mV/pH.

A more practical drift-compensation scheme is shown in Fig. 11(c), where a simple linear predictor is used to decide which data points to transmit. The data is sampled and stored in a buffer. Periodically, the drift-rate is calculated and used to predict an expected change in the data. If this is exceeded, the whole buffer should be transmitted, otherwise a single data-point will suffice. Such a scheme would provide a useful method of detecting pH *changes* in the presence of drift, and could be implemented using the on-chip microcontroller.

Note that the ultimate drift value $\Delta V_T(\infty)$ is approximately 3 times larger, and the time constant τ is 22 times shorter, than for a non-CMOS silicon nitride ISFET [18]. The larger and faster drift measured here is thought to be a result of the low-density nitride film obtained by using PECVD. CMOS processes use the relatively low temperature PECVD process to avoid damaging the underlying metallization. The non-CMOS ISFET can tolerate a high-temperature, low-pressure CVD (LPCVD) process that produces a dense nitride film, better suited to pH sensing.

The behavior of the REFET was measured in a similar manner. It was fabricated by depositing an "ion-unblocking" polymer onto the ISFET surface. The polymer is chosen to prevent hydrogen ions from reaching the pH-sensitive surface sites of the silicon nitride, while allowing the conduction of other ionic species. The PVC-based membrane composition developed by Errachid *et al.* [14] was used. As required, the pH sensitivity of the REFET was much lower at only 3.7 mV/pH. However, after a large (approximately 500 mV) initial transient, the drift-rate was approximately four times lower than for the ISFET. This means that the ISFET and REFET do not have matched electrical characteristics, so cannot be used in the differential arrangement of Fig. 6. Since the ISFET drift is caused by the in-diffusion of hydrogen ions, the creation of a REFET by the addition of a hydrogen-ion blocking membrane is not considered possible. For this reason, the complete system was tested using an external reference electrode.

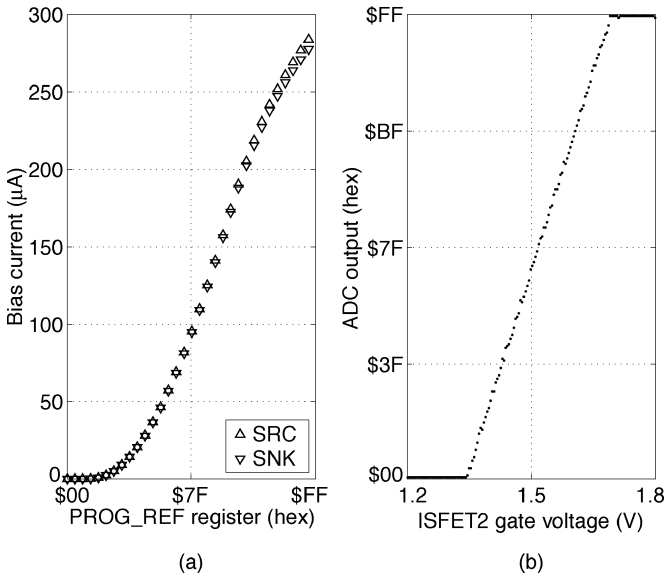

Fig. 12. Graphs showing (a) the programmable reference voltage control of source (SRC) and sink (SNK) bias currents, and (b) the overall system response to the ISFET gate voltage.

B. On-Bench System Verification

Before testing the system in solution, its behavior was verified on the bench using a packaged chip in a PCB. Fig. 12(a) shows the performance of the programmable voltage reference used to control the ISFET bias current. To measure the bias current, a program was downloaded to the MCU, that incremented the value stored in the PROG_REF register (Fig. 4). The bias currents from the $\mathrm{I_{TEST}}$ outputs were measured with a digital

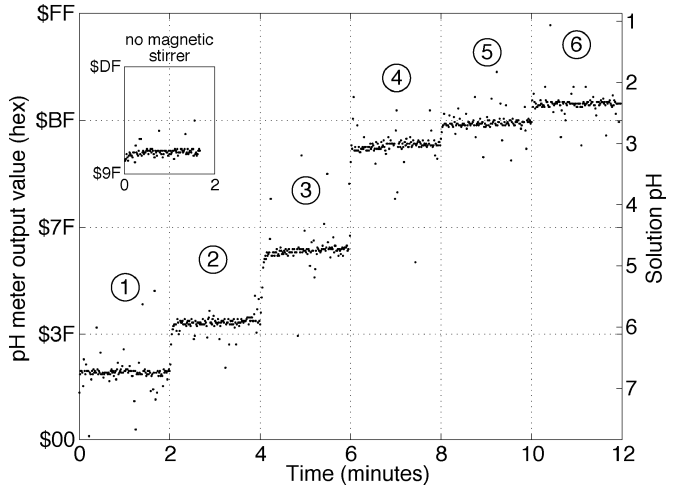

Fig. 13. Graph of the overall system-on-chip pH meter response to changes in solution pH. The inset (which is plotted at the same scale as the main graph) shows a reduction in the number of outlying data points when the magnetic stirrer was not used.

multimeter. It is clear from Fig. 12(a) that source and sink currents are almost identical up to the required current of 100 μA. In fact, they do not differ by more than 1 μA until the current exceeds 130 μA. The response of the system to the voltage on the floating electrode of the ISFET is shown in Fig. 12(b). In this case, a program was downloaded to select the output of the ISFET2_CIRCUIT block (Fig. 3) as the positive input to the instrumentation amplifier. Contact to the small pad connected to the floating electrode was made using a probe needle, which was connected to a waveform generator. The ADC output shows that the system begins to respond when the ISFET gate voltage exceeds 1.35 V, and that the overall system gain is 0.73 bits/mV.

C. In-Solution System Testing

To measure the overall response of the system to changes in solution pH, a program was downloaded to select the output of the ISFET_CIRCUIT block and the analog ground voltage as inputs to the amplifier AGIA (Fig. 3). Prior to the experiment, the chip had been conditioned in the solution for several hours to allow the threshold voltage drift to decay. The reference electrode bias was applied using a dc power supply, and the uploader software was set to collect one data-point per second. A pipette was use to add 1 M HCl to the solution at 2–min intervals. The pH of the solution was measured before and after the experiment using the Hanna pH meter. The response of the system to the changing pH is shown in Fig. 13. Although the trace is noisy, there are five distinct step changes in the value of the transmitted data. A large component of the noise is a result of the magnetic stirrer, as illustrated by the inset graph in Fig. 13, which shows data obtained with the stirrer switched off.

Fig. 13 was analyzed by considering the central 100 s of data at each of the six pH steps, in other words avoiding the data while the pH was changing. The mean values at steps ① and ⑥, together with the before and after pH readings, were used to calculate the overall pH sensitivity of 37 bits/pH. This is in good agreement with the measured ISFET sensitivity of 48 mV/pH and system response of 0.73 bits/mV. The magnetic stirrer, which was required to ensure adequate mixing, increases the standard deviation of the data by a factor of 2.5. As a result, the accuracy of the overall system was limited to approximately 0.3 pH units. Without the magnetic stirrer, the accuracy of the system could be expected to approach 0.1 pH units. Whilst there are clearly more accurate digital pH meters available, these are bench-top units, not single-chip devices suitable for use in a capsule.

Operating continuously under these conditions, the microchip consumes approximately 9 mA from a 3.3 V power supply, and the AMS transmitter consumes 8 mA. A silver-oxide cell of a suitable size for use in a capsule has a capacity of 75 mAh. This means that capsule must be powered-down for 90% of the 48 h (maximum) that it takes to pass through the human body, equivalent to one pH reading every 10 s.

V. Conclusion

A complete system-on-chip pH meter, with both analog and digital blocks, has been designed and tested. The system is controlled by a specially designed microcontroller that is fully compatible with the Motorola 6805. An additional boot-from-link facility was implemented to allow program code to be downloaded into an on-chip 2 kB SRAM. The analog subsystem made use of programmable voltage references and multiplexors to permit flexibility without the need for external connections. The overall system sensitivity was measured to be 37 bits/pH, within an operating range of 7 pH units.

The sensing element of the pH meter was a floating-electrode ISFET, that used the silicon nitride passivation layer as a pH-sensitive insulator. This allowed an ISFET to be created by an unmodified, commercial CMOS process, and without any post-processing. The ISFET was found to suffer from considerable threshold-voltage drift, which can be modeled and removed to determine the pH sensitivity. Alternatively, the drift can be compensated for using a simple linear prediction algorithm. The sensitivity was found to be 48 mV/pH, in good agreement with the only other ISFET produced by an unmodified CMOS process [8].

A REFET, with a low sensitivity of 4 mV/pH, was also created by depositing a PVC-based membrane on top of the ISFET. However, due to the difference in drift characteristics, the REFET was not able to compensate for the ISFET drift in a differential circuit. Therefore, future work will concentrate on the integration of a miniature reference electrode, and on using the microcontroller to perform real-time drift compensation.

Acknowledgment

The authors would like to acknowledge the assistance of Dr. A. Glidle at the University of Glasgow and the design engineers at austriamicrosystems.

References

[1] A. Hierlemann and H. Baltes, "CMOS-based chemical microsensors," *Analyst*, vol. 128, pp. 15–28, 2003.

[2] C. Hagleitner, A. Hierlemann, D. Lange, A. Kummer, N. Kerness, O. Brand, and H. Baltes, "Smart single-chip gas sensor microsystem," *Nature*, vol. 414, pp. 293–296, 2001.

[3] J. Pandolfino, J. Ritcher, T. Ours, R. Jason, M. Guardino, J. Chapman, and P. Kahrilas, "Ambulatory esophageal pH monitoring using a wireless system," *Am. J. Gastroenterol.*, 2003.
[4] Y. Sasaki, R. Hada, H. Nakajima, S. Fukada, and A. Munakata, "Improved localizing method of radiopill in measurement of entire gastrointestinal pH profiles: colonic luminal pH in normal subjects and patients with Crohn's disease," *Am. J. Gastroenterol.*, vol. 92, no. 1, pp. 114–118, 1997.
[5] A. Press, I. Hauptmann, B. Fuchs, M. Fuchs, K. Ewe, and G. Ramadori, "Gastrointestinal pH profiles in patients with inflammatory bowel disease," *Aliment. Pharmacol. Ther.*, vol. 12, pp. 673–678, 1998.
[6] J. Enemark, G. Peters, and R. Jørgensen, "Continuous monitoring of rumen pH—a case study with cattle," in *J. Vet. Med. A*, 2003, vol. 40, pp. 62–66.
[7] E. Johannessen, L. Wang, L. Cui, T. Tang, M. Ahmadian, A. Astaras, S. Reid, A. Murray, B. Flynn, S. Beaumont, D. Cumming, and J. Cooper, "Implementation of multichannel sensors for remote biomedical measurements in a microsystem format," *IEEE Trans. Biomed. Eng.*, vol. 51, no. 3, pp. 525–535, Mar. 2004.
[8] J. Bausells, J. Carrabina, A. Errachid, and A. Merlos, "Ion-sensitive field-effect transistors fabricated in a commercial CMOS technology," *Sens. Actuators, B*, vol. 57, pp. 56–61, 1999.
[9] P. Hammond, D. Ali, and D. Cumming, "Design of a single-chip pH sensor using a conventional 0.6 μm CMOS process," *IEEE Sensors J.*, no. 6, pp. 706–712, Dec. 2004.
[10] L. Chirwa, P. Hammond, S. Roy, and D. Cumming, "Electromagnetic radiation from ingested sources in the human intestine between 150 MHz and 1.2 GHz," *IEEE Trans. Biomed. Eng.*, vol. 50, no. 4, pp. 484–492, Apr. 2003.
[11] L. Ravezzi and P. Conci, "ISFET sensor coupled with CMOS read-out circuit microsystem," *Inst. Elect. Eng. Electron. Lett.*, vol. 34, no. 23, pp. 2234–2235, 1998.
[12] H. Suzuki, H. Shiroishi, S. Sasaki, and I. Karube, "Microfabricated liquid junction Ag/AgCl reference electrode and its application to a one-chip potentiometric sensor," *Anal. Chem.*, vol. 71, pp. 5069–5075, 1999.
[13] I.-Y. Huang and R.-S. Huang, "Fabrication and characterization of a new planar solid-state reference electrode for ISFET sensors," *Thin Solid Films*, vol. 406, pp. 255–261, 2002.
[14] A. Errachid, J. Bausells, and N. Jaffrezic-Renault, "A simple REFET for pH detection in differential mode," *Sens. Actuators, B*, vol. 60, no. 43–48, 1999.
[15] M. Chudy, W. Wróblewski, and Z. Brzózka, "Toward REFET," *Sens. Actuators, B*, vol. 57, pp. 47–50, 1999.
[16] T. Matsuo and M. Esashi, "Methods of ISFET fabrication," *Sens. Actuators*, vol. 1, pp. 77–96, 1981.
[17] P. Hammond and D. Cumming, "Encapsulation of a liquid-sensing microchip using SU-8 photoresist," *Microelectron. Eng.*, vol. 73–74, pp. 893–897, 2004.
[18] S. Jamasb, S. Collins, and R. Smith, "A physical model for drift in pH ISFETs," *Sens. Actuators, B*, vol. 49, pp. 146–155, 1998.
[19] J. Kakalios, R. Street, and W. Jackson, "Stretched-exponential relaxation arising from dispersive diffusion of hydrogen in amorphous silicon," *Phys. Rev. Lett.*, vol. 59, no. 9, pp. 1037–1040, 1987.
[20] W. Press, B. Flannery, S. Teukolsky, and W. Vetterling. (1993) *Numerical Recipes in C: The Art of Scientific Computing* (2nd ed.) [Online] Available: http://www.library.cornell.edu/nr/bookcpdf.html

Paul A. Hammond received the M.Eng. degree from the University of Cambridge, Cambridge, U.K., in 1999, and the Ph.D. degree from the University of Glasgow, Glasgow, U.K., in 2004.

Between degrees he worked for STMicroelectronics as a CMOS analog circuit designer. He is currently a Research Assistant in the Department of Electronics at the University of Glasgow. His interests include the use of system-on-chip integration for sensing applications.

Danish Ali received the B.A. and M.A. degrees in natural sciences from the University of Cambridge, Cambridge, U.K. in 1988 and 1992. He received the Ph.D. degree in microelectronics from the Cavendish Laboratory at Cambridge in 1994. I

n 1995 he joined Philips Research Laboratories in Redhill, U.K., initially in the cordless communications group but more recently in the wireless group. There he has been doing research into circuit design and system optimization for wireless communication devices. His interests include baseband signal processing and analog-to-digital conversion.

David R. S. Cumming (M'97) received the B.Eng. degree from the University of Glasgow, Glasgow, U.K., in 1989 and the Ph.D. degree from Cambridge University, Cambridge, U.K., in 1993. He has worked variously on mesoscopic device physics, RF characterization of novel devices, fabrication of diffractive optics for optical and submillimeter wave applications, diagnostic systems, and microelectronic design. He is presently a Professor and EPSRC Advanced Research Fellow in Electronics and Electrical Engineering at the University of Glasgow where he leads the Microsystem Technology Research Group.